ISSN (Print) 1226-1750
ISSN (Online) 2233-6656
Journal of Magnetics 30(4), 876-880 (2025) https://doi.org/10.4283/JMAG.2025.30.4.876

Feasibility of a CsI(Tl)-GAPD Line Radiation Detector for Seafood Contamination Detection

Minseo Cha[1], Suhan Choi[2], Junho Kang[2], Donggeun Roh[2], and Jihoon Kang[1,2,3]*

[1]*Department of Biomedical Engineering, Chonnam National University, Yeosu 59626, Republic of Korea*
[2]*Interdisciplinary Program of Biomedical Engineering, Chonnam National University, Yeosu 59626, Republic of Korea*
[3]*Research Center for Healthcare-Biomedical Engineering, Chonnam National University, Yeosu 59626, Republic of Korea*

(Received 7 November 2025, Received in final form 17 December 2025, Accepted 17 December 2025)

This paper presents the design and performance evaluation of a field-deployable, real-time, multi-channel line radiation detector for imaging radioactive contamination in seafood. The detector integrates scintillator arrays made of thallium-doped cesium iodide (CsI(Tl)) with Geiger-mode avalanche photodiodes (GAPDs) to enable spatially resolved gamma-ray detection. This detector consists of 128 channels arranged in a 4 × 32 configuration, providing a total active area of 98.24 mm × 12.28 mm. The CsI(Tl) scintillator is configured as a 4 × 4 array, with each pixel measuring 3 × 3 × 10 mm³ and wrapped in a TiO_2 reflector. The GAPD array possesses the same 4 × 4 geometry, and each pixel has a sensitive area of 3.07 × 3.07 mm². The photon detection efficiency at 540 nm is approximately 30%, with a gain on the order of 10^6. Signals from 32 individual GAPD channels are multiplexed into four analog outputs via resistive charge division (RCD), enabling the gamma-ray interaction position to be extracted. Subsequently, the multiplexed signals are amplified by a two-stage inverting amplifier with an overall gain of approximately 20 and digitized by a data acquisition system for storage and analysis. Performance is evaluated using a fish sample containing an embedded Na-22 point source, and the source position is reconstructed as heatmaps obtained from line scans at 17 positions with 12 mm spacing. The detector achieves an average energy resolution of 15.9 ± 2.0% at 511 keV, demonstrating uniform performance across all 128 channels. The heatmaps reveal high counts at scan positions corresponding to the Na-22 source within the fish sample, clearly resolving the spatial distribution of gamma rays. These results indicate that the proposed detector can detect and image radioactive contamination during seafood inspection, and future work will investigate the feasibility of a magnetic resonance-compatible radiation detector based on gamma-ray position discrimination.

Keywords : CsI(Tl)-GAPD, line radiation detector, resistive charge division, MR-compatible radiation detector

1. Introduction

Following the 2011 Fukushima nuclear disaster, the demand for radioactivity testing of seafood has substantially increased. However, conventional laboratory-based approaches possess significant limitations. High-purity germanium spectrometers, widely regarded as the standard for radionuclide detection, incur prohibitively high operational costs, require specialized maintenance and expertise, and often necessitate destructive sample preparation. In addition, the inability of these spectrometers to efficiently process large batches of samples restricts testing to centralized facilities, thereby hindering real-time on-site screening and the comprehensive inspection of seafood products [1, 2]. Consequently, this urgently necessitates a detection technology that can simultaneously provide low background noise and high detection efficiency to enable accurate on-site assessment of radionuclide distribution [3, 4].

To address these limitations, a multi-channel line radiation detector that combines thallium-doped cesium iodide (CsI(Tl)) scintillators with Geiger-mode avalanche photodiodes (GAPDs) is proposed in this study [5]. CsI(Tl) was selected as the primary scintillator material owing to its high light yield, excellent mechanical stability, and lower hygroscopicity than alternatives such as NaI(Tl), ensuring reliable operation across diverse field environments [6].

*Corresponding author: Tel: +82-61-659-7363
Fax: +82-61-659-7369, e-mail: ray.jihoon.kang@gmail.com

GAPDs were employed as the photosensor component owing to their inherently high gain, compact form factor, and excellent scalability, critical attributes for multi-channel detector configurations designed for real-time analysis [7-9]. In addition, GAPD-based detector modules have been widely investigated for use in magnetic resonance environments, including positron emission tomography magnetic resonance imaging and photon-counting detector systems [10-12]. Moreover, resistive charge division (RCD) technology was implemented to efficiently multiplex signals from 128 individual channels while preserving both positional and energy information [13-15]. The multiplexed signals were subsequently amplified using a two-stage inverting amplifier with an overall gain of approximately 20, and a data acquisition (DAQ) system subsequently converted the analog signals to digital data for storage and analysis.

The proposed 128-channel line detector can directly detect radioactivity in real time at deployment sites, thereby facilitating the comprehensive inspection of seafood batches and overcoming the operational constraints of traditional laboratory protocols. This paper presents the conceptual design, hardware implementation, and comprehensive performance characterization of the developed 128-channel (4 × 32) CsI(Tl)–GAPD-based line radiation detector system and demonstrates the practical viability of this system for real-time on-site radioactivity assessment of seafood.

2. Materials and Methods

2.1. Design concept

Each CsI(Tl) scintillator present in the sub-detector units of the line radiation detector was arranged in a 4 × 4 array, with each pixel measuring 3 × 3 × 10 mm³. Additionally, a TiO_2 reflector was placed between adjacent scintillator pixels. The GAPD array had the same 4 × 4 configuration as the CsI(Tl) array and provided an active area of 3.07 × 3.07 mm² per pixel. At the effective emission wavelength of CsI(Tl), i.e., 540 nm, the photon detection efficiency of the GAPD was approximately 30%, and the device provided a signal gain of approximately 10^6. The CsI(Tl) crystals and the GAPD array were optically coupled using BC-630 optical grease to reduce the refractive-index mismatch between the coupling surfaces of the crystals and the array, and minimize light loss due to reflection by eliminating air gaps, as shown in Fig. 1.

Two 4 × 4 sub-detector units were arranged horizontally to construct a detector module with a 4 × 8 configuration (32 channels). External light contamination was prevented by wrapping the detector module in white Teflon tape (reflector) and black insulating tape (light seal).

Readout of the 4 × 8 detector module is implemented using an RCD network, as depicted in Fig. 2. The RCD network multiplexed signals from 32 individual scintillation channels into four analog outputs, i.e., A, B, C, and D. The position of each event was calculated using Eqs. (1) and (2).

$$X = \frac{A + B}{A + B + C + D'} \tag{1}$$

$$Y = \frac{A + C}{A + B + C + D'} \tag{2}$$

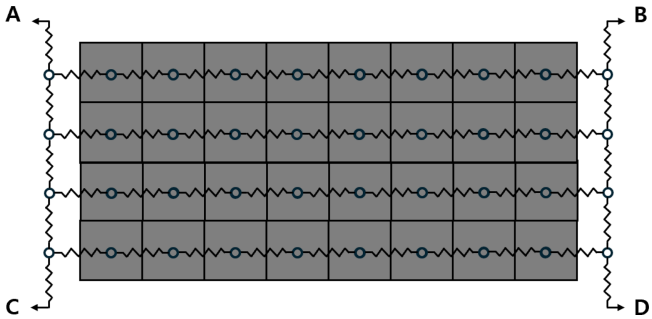

Fig. 2. Schematic of the 4 × 8 RCD network to enable multiplexed signal readout with four output nodes (A, B, C, and D).

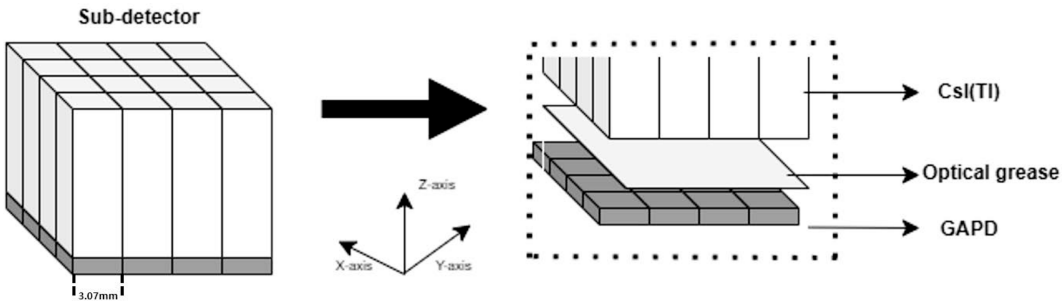

Fig. 1. Schematic diagram of the sub-detector structure, consisting of a 4 × 4 CsI(Tl) scintillator array optically coupled to a 4 × 4 GAPD array using optical grease.

Where X and Y represent the row and column positions of the radiation event, respectively. The sum A+B+C+D corresponds to the total energy deposited by the event. These position calculations can be used to discriminate between the 32 individual scintillation crystals within each detector module.

Subsequently, four identical 4 × 8 detector modules were arranged in series to construct a complete line radiation detector with a 4 × 32 configuration (128 channels in total). The active detection area obtained was 98.24 mm (horizontal) × 12.28 mm (vertical), thereby enabling line scanning of the radiation distribution with a pixel resolution matching the dimensions of the individual scintillation crystals (3 × 3 mm²).

2.2. Experimental setup

The performance of the proposed line radiation detector was evaluated using a seafood sample, approximately 200 mm in length, at the center of which a Na-22 point source with an activity of 3.15 MBq was inserted. The detector was positioned parallel to the sample surface at 60 mm distance. All measurements were obtained inside a black shielding box to completely block external light.

To implement line scanning, the sample was translated in 12 mm steps, chosen to match the effective vertical resolution of the detector, i.e., approximately 12 mm, to cover the entire 200-mm sample length. A total of 17 measurement positions, therefore, spanned approximately 204 mm along the sample axis, and data were acquired over 600 s at each position.

Signals generated in the detector were multiplexed into four channels, i.e., A, B, C, and D, by the RCD network, and the multiplexed outputs were routed to a preamplifier via a flat-flex cable connector. An AD8012 operational amplifier in the dual inverting configuration was used as a preamplifier, providing an overall voltage gain of approximately 20. Subsequently, the amplified signals were digitized by a data acquisition (DAQ) system and stored for offline analysis. The DAQ parameters were set to an offset of approximately 100 mV, a trigger level of 250 mV, and a dead time of 1800 ns.

2.3. Performance evaluation

The four-channel signals, i.e., those obtained from A,

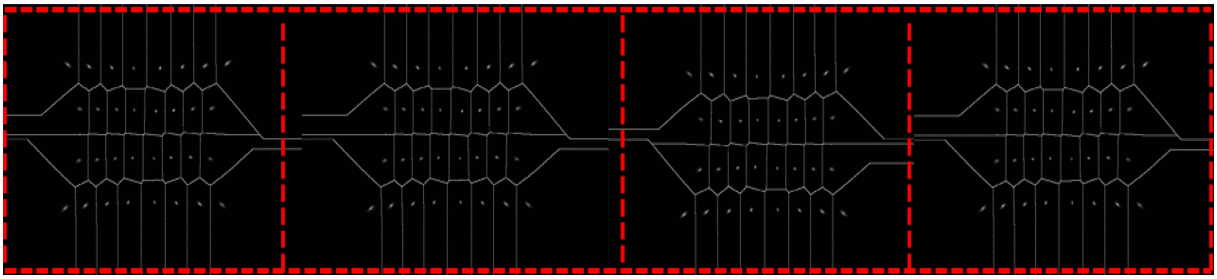

Fig. 3. (Color online) Flood map of the 4 × 32 CsI(Tl)–GAPD line radiation detector obtained using a Na-22 source after watershed segmentation.

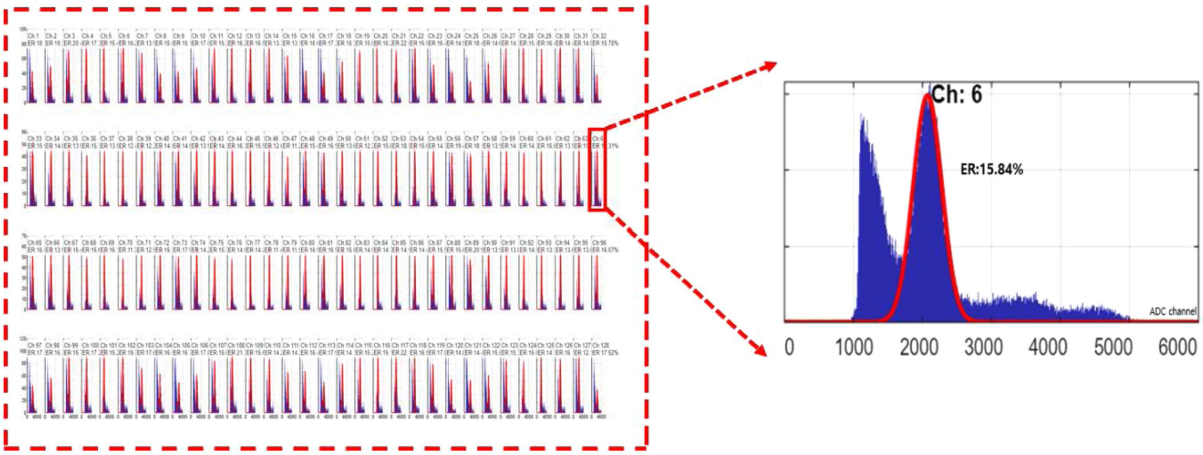

Fig. 4. (Color online) Energy spectra of all the channels obtained using the CsI(Tl)–GAPD line radiation detector. The inset depicts a representative result of photopeak fitting corresponding to a single channel. *ER: energy resolution.

B, C, and D, acquired from the RCD network, were converted to X–Y spatial coordinates using Eqs. (1) and (2) and subsequently reconstructed into a two-dimensional flood map, such that the signal distribution across the detector can be visualized. In addition, watershed segmentation was applied to distinguish all 128 individual detector channels.

Energy spectra of the individual detector channels were generated as histograms to identify the 511 keV photopeak obtained from the Na-22 source, and the energy resolution was subsequently determined via Gaussian fitting of the photopeak.

To localize radiation, an energy window of ±15% centered on the 511 keV photopeak was defined, and events falling within this window were visualized as a heatmap to evaluate the spatial response characteristics of the detector.

3. Results

Fig. 3 displays the two-dimensional flood map acquired from measurements conducted on the Na-22 point source. Application of the watershed algorithm resolved all 128 channels in the 4 × 32 array configuration, with individual channels distinctly separated. Fig. 4 depicts the energy spectra of the individual detector channels, with the 511 keV photopeak from the Na-22 source clearly demarcated. The detector achieved an average energy resolution of (15.9 ± 2.0)% (full width at half maximum (FWHM)) across all channels. Fig. 5 illustrates the spatial detection performance of the line radiation detector. The reconstructed heatmap exhibited maximum intensity in the region corresponding to the source location and considerably reduced intensity in the surrounding regions, confirming accurate spatial localization.

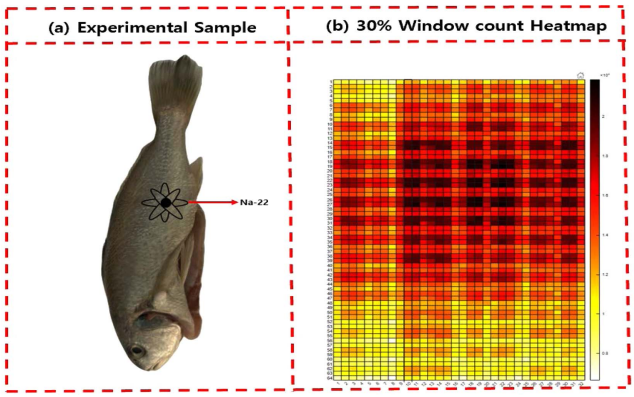

Fig. 5. (Color online) Spatial detection of radioactive contamination in the fish sample: (a) experimental sample with an embedded Na-22 point source and (b) count distribution heatmap obtained via line scanning.

4. Discussion and Conclusion

This paper presents the design and performance evaluation of a CsI(Tl)–GAPD-based line radiation detector for radioactivity inspection of seafood. The detector acquires signals from 128 individual channels, multiplexed via an RCD network, enabling the simultaneous extraction of energy and spatial position information for radiation events. A CsI(Tl) scintillator with low sensitivity to natural background radiation, low hygroscopicity, and high mechanical strength was employed to better reflect field deployment conditions. Scintillation light was read out using GAPDs and further processed using a preamplifier stage to effectively detect radiation within seafood samples.

The 511 keV gamma-ray photopeak obtained from the Na-22 source was clearly identified in all detector channels, and the system achieved an average energy resolution of (15.9 ± 2.0)% (FWHM) across all 128 channels. Although this value is somewhat inferior to those reported in previous studies related to CsI(Tl)–GAPD. This is possibly owing to the extended detector array and the specific characteristics of the radioactivity inspection environment related to seafood; however, this is sufficient to clearly resolve the 511 keV photopeak [16]. Therefore, the measured performance is considered adequate to construct an imaging system to detect radioactive contamination in seafood. The reconstructed heatmap revealed that the maximum count density was concentrated around the lower abdominal region of the sample, at which the Na-22 point source was inserted, whereas positions far from the source exhibited reduced count levels. These line scanning results demonstrate that the proposed detector can detect and localize radioactive contamination within seafood specimens.

This study, however, has several limitations. First, a fully realistic inspection environment for seafood could not be implemented. Measurements were obtained by embedding a radiation source inside the seafood sample, yielding higher activity levels than those typically observed in real contaminated seafood; therefore, further studies using reduced-activity sources are required to ensure realistic evaluation. Second, the present analysis primarily relied on qualitative evaluation of the reconstructed count distributions and failed to provide a comprehensive set of quantitative performance metrics.

Future studies will integrate radiation distribution data with optical and thermal imaging to develop a real-time monitoring system to simultaneously visualize the sample

morphology and internal radionuclide distribution. Moreover, a systematic quantitative evaluation of the detector's spatial-localization performance, based on representative resolution and contrast metrics, will be conducted in future work. In addition, by enhancing the algorithms used for gamma-ray position analysis and conducting high-precision measurements, the feasibility of a magnetic resonance-compatible radiation detector will be further investigated. The proposed detector can potentially be applied in various fields, including seafood radioactivity screening, radiation imaging systems, and monitoring in magnetic resonance environments.

Acknowledgment

This research was supported by the National Research Foundation of Korea (NRF) grant funded by the Korean government (MSIT) (No. RS-2023-00243325), and by the Regional Innovation System & Education (RISE) program through the Jeollanamdo RISE Center, funded by the Ministry of Education (MOE) and Jeollanamdo, Republic of Korea (No. 2025-RISE-14-007).

The authors would like to thank Enbiogene Co., Ltd. for providing the Fish Imaging Chamber (FIC) employing petrochemical-derived water-shielding materials, as well as for their valuable technical support. We also thank Chun-seop Kim for helpful discussions.

References

[1] M. W. Cooke, M. Trudel, H. J. Gurney-Smith, J. P. Kellogg, J. T. Cullen, B. B. A. Francisco, J. F. Mercier, and J. Chen, J. Environ. Radioact. **251-252**, 106934 (2022).

[2] S. Merz, K. Shozugawa, and G. Steinhauser, Environ. Sci. Technol. **49**, 2875 (2015).

[3] A. Bross, E. C. Dukes, S. Hansen, A. Pla-Dalmau, and P. Rubinov, arXiv:2307.04828 (2023).

[4] IAEA, Determination of Radionuclides in Sea Water, Sediment and Biota Samples, Analytical Quality in Nuclear Applications Series AQ-59, International Atomic Energy Agency, Vienna, Austria (2018).

[5] R. Hawrami, Y. Zhou, and G. Cho, arXiv:2106.10403 (2021).

[6] K. F. Suzart, A. F. Velo, M. M. Hamada, M. C. C. Pereira, and C. H. Mesquita, Braz. J. Radiat. Sci. **09-01A**, 01 (2021).

[7] G. S. M. Ahmed, J. Marton, M. Schafhauser, K. Suzuki, and P. Bühler, J. Instrum. **4**, P09004 (2009).

[8] H. S. Yoon, G. B. Ko, S. I. Kwon, C. M. Lee, M. Ito, I. C. Song, D. S. Lee, S. J. Hong, and J. S. Lee, J. Nucl. Med. **53**, 608 (2012).

[9] H. W. Park, M. S. Yi, and J. S. Lee, Biomed. Eng. Lett. **12**, 263 (2022).

[10] S. J. Lee and C. H. Baek, J. Magn. **30**, 448 (2025).

[11] G. R. Kim, J. H. Kwak, and S.-J. Lee, J. Magn. **30**, 442 (2025).

[12] D. Kim, H. Lee, and S.-J. Lee, J. Magn. **25**, 601 (2020).

[13] J. Kang, Y. Choi, K. B. Kim, J. H. Jung, W. Hu, and Y. H. Chung, IEEE Trans. Nucl. Sci. **61**, 1059 (2014).

[14] J. Kang, Y. Choi, K. J. Hong, W. Hu, J. H. Jung, Y. S. Huh, H. Lim, and B. T. Kim, J. Instrum. **6**, P08012 (2011).

[15] J. Kang, Y. Choi, K. J. Hong, J. H. Jung, W. Hu, Y. S. Huh, H. Lim, and B. T. Kim, Med. Phys. **37**, 5655 (2010).

[16] S. Choi, D. Roh, and J. Kang, J. Magn. **29**, 523 (2024).